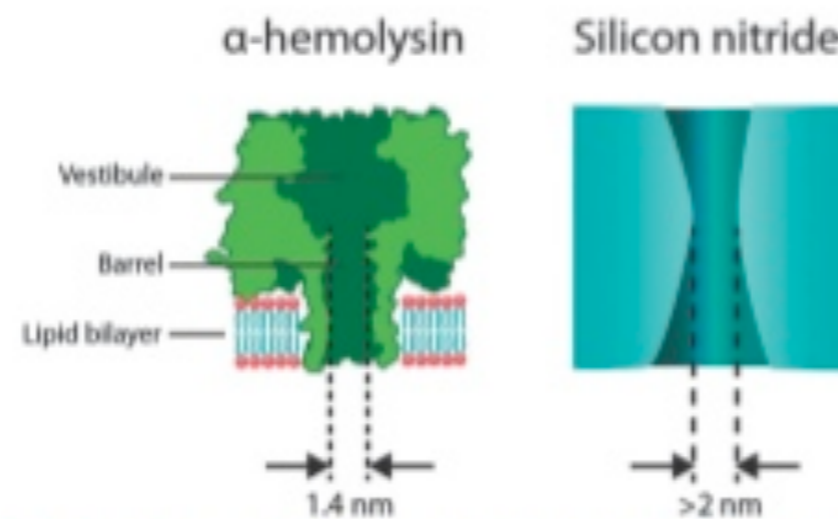


# Solid State Nanopores in Biosensing

# Applications

- Ionic current blockade for nucleic acid sequencing
- Nanopore force spectroscopy for molecular interactions
- Fluidic transistors for molecular capture
- Zero-mode wave guides for molecular characterization

# Current Blockade Setup



**Fig. 1** (left) An  $\alpha$ -hemolysin biological nanopore embedded in a lipid bilayer membrane. This protein has been adopted for *in vitro* nanopore sensing applications due to its ability to permit the passage of small solutes and relatively large macromolecules in a linear conformation such as DNA. Furthermore,  $\alpha$ -hemolysin is amenable to protein engineering that can provide single point mutations in the vestibule or the barrel that can later be used in the conjugation of recognition elements. (right) A cross-sectional illustration of a typical solid-state nanopore fabricated in a silicon nitride membrane. The pore diameter can be finely tuned and typically ranges from 2 nm upwards. The nanopore shape can approximate an hourglass, cylinder, or cone, depending on the fabrication methods. In cylindrical nanopores, the depth is defined by the thickness of the membrane and typically takes on dimensions of approximately 10–200 nm. Silicon nitride nanopores are easily amenable to modification by using either surface chemistry or semiconductor processing techniques.

# Current Blockade Results

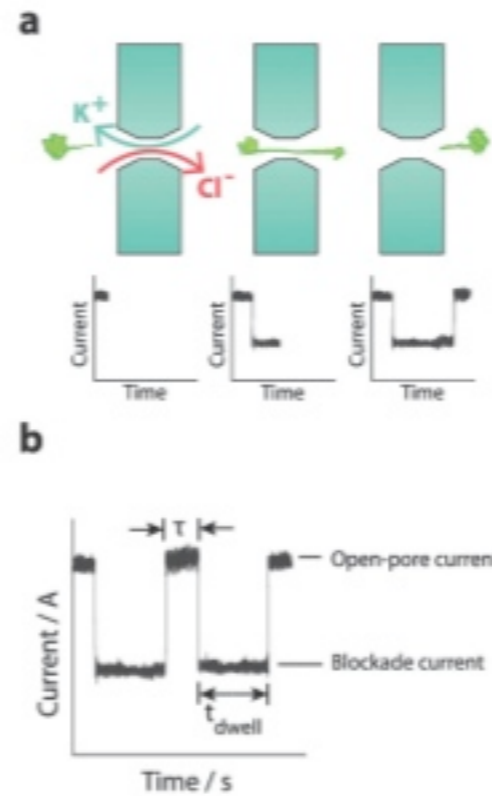


**Fig. 2** (a) The schematic shows the ionic current recorded as a function of time and the interpretation of the analyte translocation process. The steady-state ionic current is decreased when the analyte is translocated through the pore and then re-established when the molecule exits the pore. (b) Four parameters are generally used to characterise the translocation process: (i) The blockade duration or the time the molecule spends in the nanopore ( $t_{\text{block}}$ ). (ii) The amplitude of the blockade current (i.e. difference between open-pore current and the blockade current). (iii) The time between translocation events ( $\tau$ ). (iv) The capture rate defined as the number of translocation events per unit time. All parameters are directly dependent on the applied bias, and nanopore geometry as shown in eqn (1) whilst (ii) and (iv) are also dependant on the analyte concentration.

# NPFS Setup

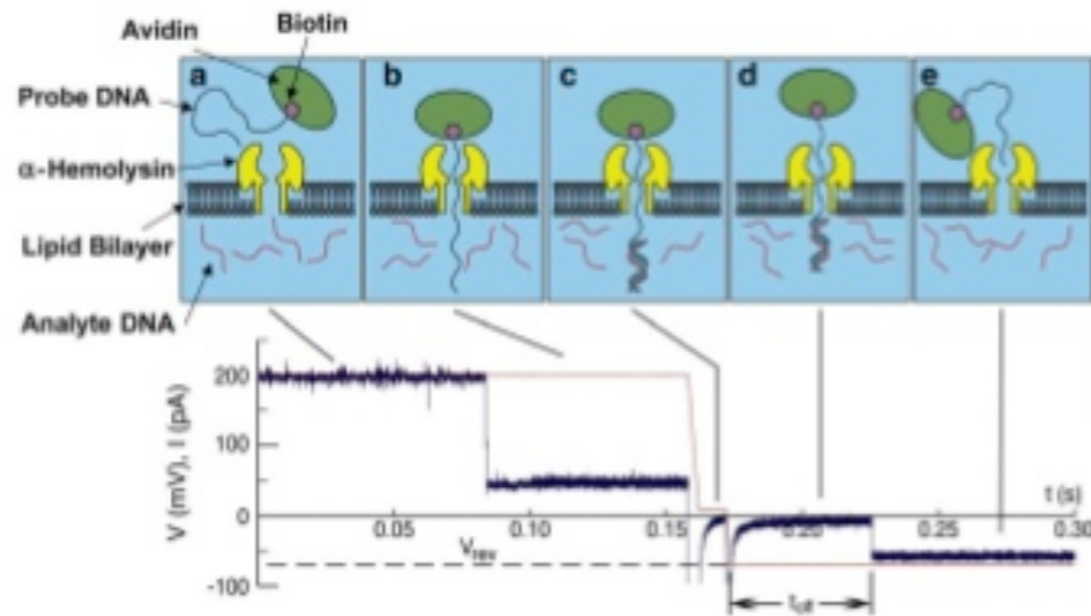
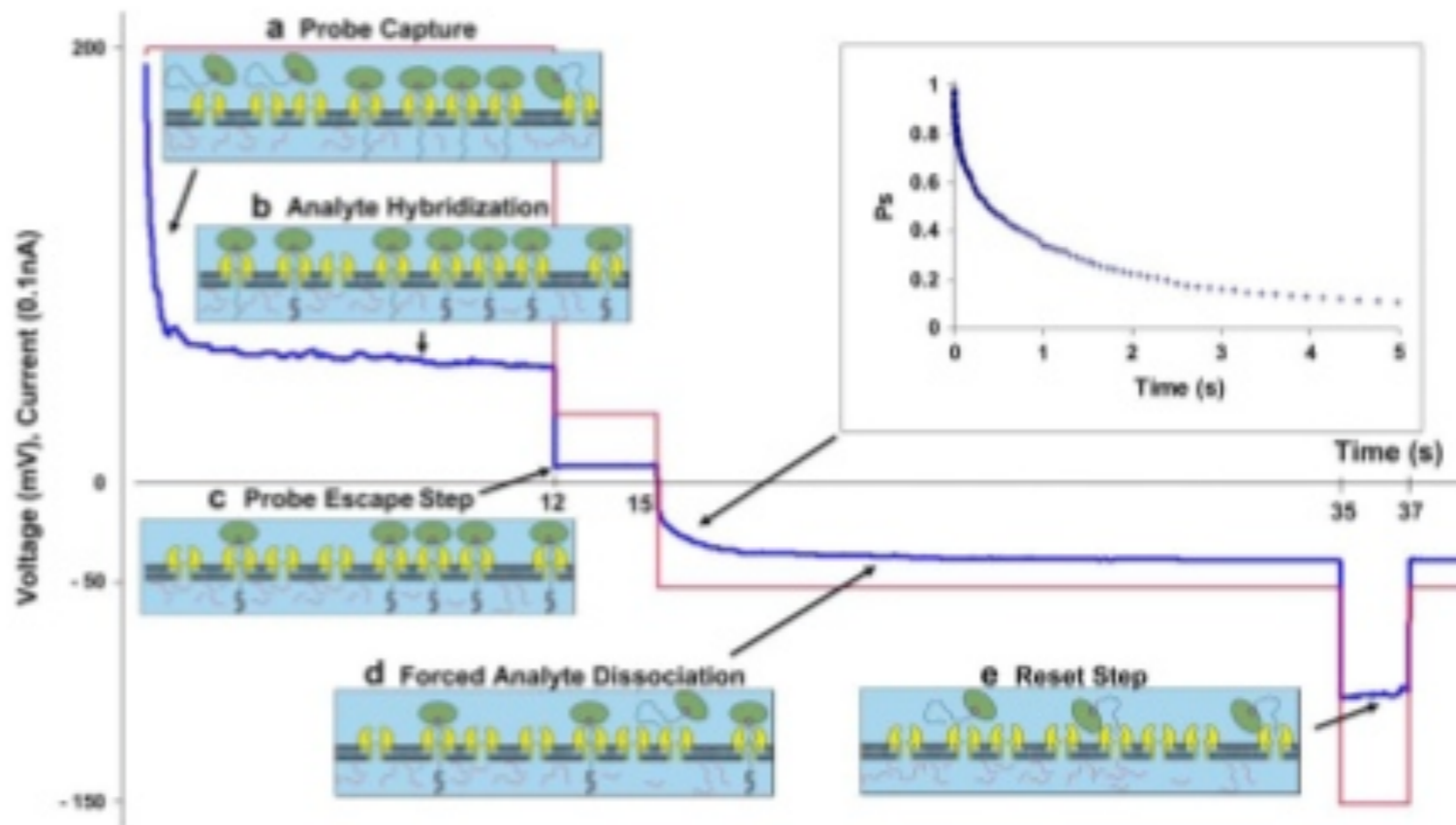
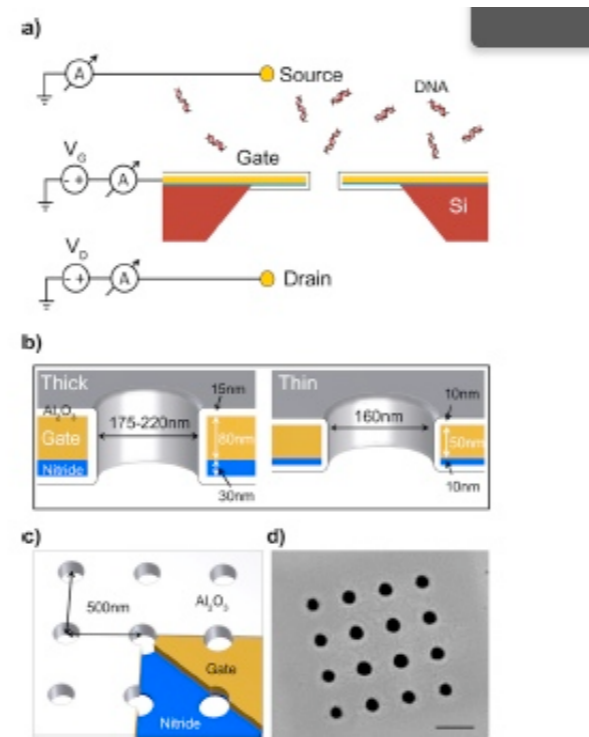


FIGURE 1 Single molecule force spectroscopy. Force is applied through electrophoretic control of a DNA homopolymer traversing a single  $\alpha$ -HL pore and prevented from translocating by an avidin anchor. Dissociation time of a DNA duplex under force is measured for a range of applied forces. Reproduced with permission from *Biophysical Journal* (5).

# NPFS Results



# Nanofluidic Transistor Setup



**Figure 1.** Schematics and SEM image of the nanofluidic transistor. (a) NFT is in buffered 10 mM NaCl solution. The source well is grounded through a Au or a Ag/AgCl electrode and contains 2.5 nM of 100 bp DNA fragments. The drain well has +800 mV applied. (b) Two versions of the NFT were made, thick and thin. The thick NFT is designed to have a 140 nm thick membrane composed of 30 nm thick SiN<sub>x</sub> and 80 nm of gate material surrounded by 15 nm of Al<sub>2</sub>O<sub>3</sub> deposited by ALD. The thin NFT has an 80 nm thick membrane composed 10 nm thick SiN<sub>x</sub> and 50 nm of gate material surrounded by 10 nm Al<sub>2</sub>O<sub>3</sub>. (c) Pores are milled by FIB 500 nm apart in a 4 × 4 square pattern. (d) SEM image of an array. The scale bar is 500 nm.

# Multi-NPFS Results

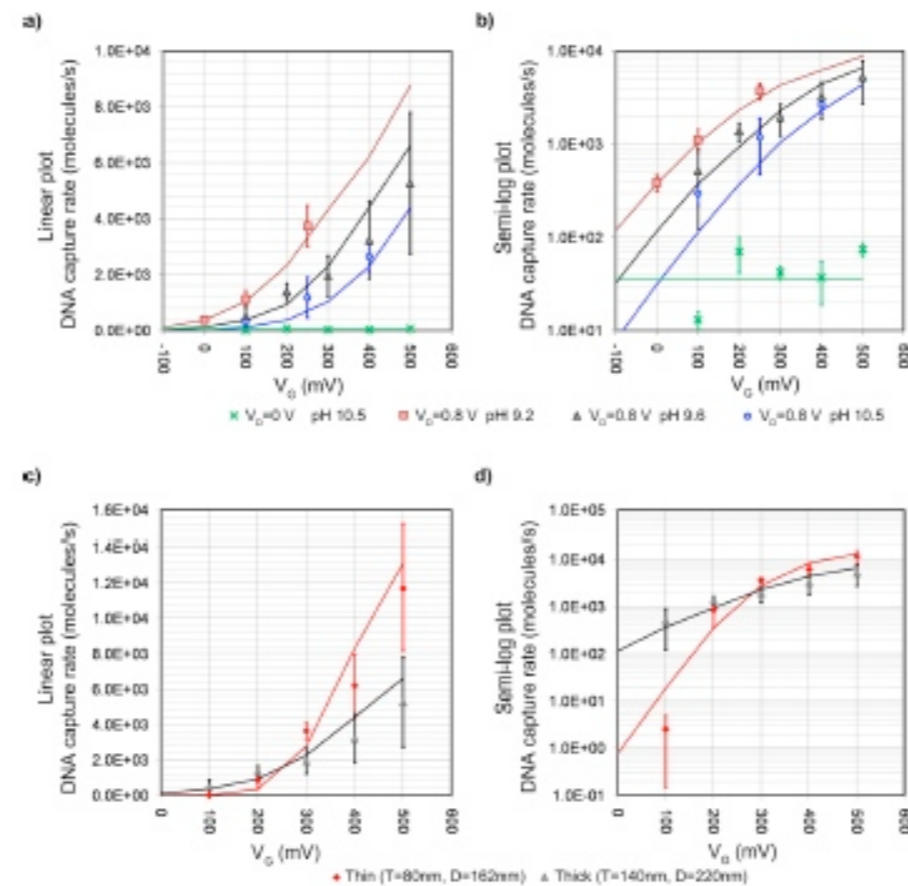


Figure 2. Experimental results of DNA capture rate vs  $V_G$  compared to simulation. The markers represent the experimental results. The error bars are standard deviations of experimental results. Simulated results are shown as solid lines. (a) Plot of DNA capture rate vs  $V_G$  for various solution pHs of the thick NFT devices. When  $V_G = +800$  mV,  $V_G$  is able to control DNA capture rate of the nanofluidic transistor (NFT) by altering the counterion concentration. Further, the solution pH also alters pore surface charge. Thus, changing pH results in shifting the DNA capture threshold. In simulations, this pH dependence is modulated by assigning different surface charge densities (Supporting Information Table S3). We also performed the experiment when  $V_G = 0$  V, the net translocation rate is small, ca. 50/s. (b) Semilog plot of the results shown in panel (a). (c) Plot of DNA capture rate vs  $V_G$  of NFTs before and after the design revision to enhance modulation. Both devices are in solution with pH 9.5. The thin device, with smaller diameter pores and a thinner gate dielectric film, has enhanced gate control. The application of the same  $V_G$  across a thinner membrane results in larger transmembrane electric field, as well. This results in strong or relative EOF that can turn the device off at low  $V_G$  and have larger capture rate at high  $V_G$ . (d) Semilog plot of the results shown in panel (c).

# Possibilities For NRG & SiMPore

- Backfilling FIB nanopores - novel shape & properties
- pnc-Si windows in NPFS - small diameter, controlled #s of exposed pores
- pnc-Si nanofluidic transistors - size-binning complex samples